ACS Macro Letters

Letter

pubs.acs.org/macroletters

Free-Standing Films from Aqueous Dispersions of Lysozyme, Single-Walled Carbon Nanotubes, and Polyvinyl Alcohol

A. Gloria Nyankima, Daniel W. Horn, and Virginia A. Davis*

Department of Chemical Engineering, Auburn University, 212 Ross Hall, Auburn, Alabama 36849, United States

ABSTRACT: Transparent antibacterial films were produced by casting concentrated dispersions of lysozyme (LSZ), single-walled carbon nanotubes (SWNTs), and polyvinyl alcohol (PVA). The initial SWNT dispersion state had a significant influence on the films' mechanical properties. Films containing 9 wt % bundled SWNTs had six times higher Young's modulus than control films produced without SWNTs. Removal of SWNT bundles by centrifugation prior to concentrating the dispersions resulted in films that contained only 4.5 wt % SWNT but had over eight times higher Young's modulus than the control films.

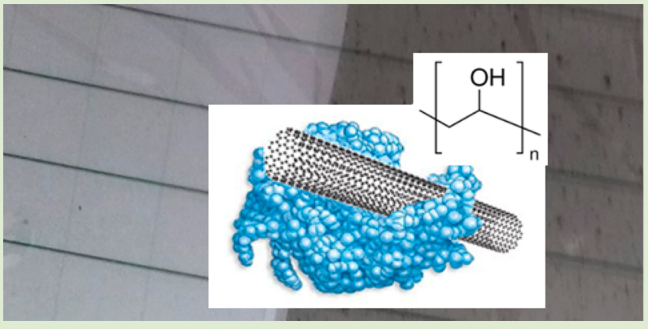

There is growing interest in combining the mechanical properties of single-walled carbon nanotubes (SWNTs) with biological materials such as DNA and enzymes.[1−8] One enzyme of particular interest is lysozyme (LSZ), a naturally abundant enzyme that lyses Gram-positive bacteria such as *Staphylococcus aureus* and *Micrococcus lysodeikticus*. LSZ is used commercially for its antibacterial properties in several applications including toothpaste,[9] mouthwash,[10,11] and cheese coatings.[12] In previous work, layer-by-layer assembly of aqueous dilute supernatants of LSZ−SWNT and double-stranded DNA−SWNT resulted in strong, antibacterial coatings whose layer thickness could be controlled within 1.6 nm.[3] The SWNT concentration in those dispersions was on the order of 10^{-3} wt %. Casting free-standing, large area films from such dilute dispersions can be impractical. However, concentrating the LSZ−SWNT dispersions resulted in significant aggregation. We report that the addition of polyvinyl alcohol (PVA) to LSZ−SWNT dispersions increases dispersion stabilty and enables casting of transparent, mechanically robust, antibacterial films. PVA was chosen because it is a water-soluble polymer that provides elasticity and is known to fill voids in SWNT films and fibers.[13] As described in previous work,[3,6,14] LSZ−SWNT mixtures contain a combination of individually dispersed SWNTs as well as bundles and aggregates. Mixture centrifugation removes aggregates and large bundles and results in a supernatant containing predominantly individual SWNTs. In this work, both mixture and supernatant dispersions were mixed with 5 wt % aqueous PVA, concentrated by evaporation, and cast into films (see Experimental Section). Films produced from the initial mixtures had macroscopic visible aggregates, while films produced from the supernatants were transparent with no optical evidence of SWNT aggregation (see Figure 1). The ternary interactions between PVA, SWNT, and LSZ are not yet well understood. However, it is known that SWNT and LSZ associate through $\pi-\pi$ stacking and hydrophobic interactions primarily between the LSZ's tryptophan residue and the aromatic SWNT sidewall.[6] To ascertain interactions between LSZ, SWNT, and PVA within the solid films, ATR-FTIR spectroscopy was used.

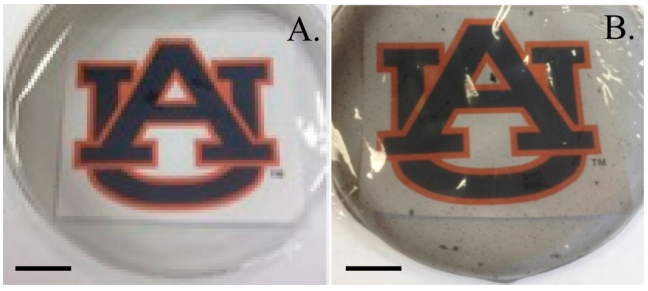

Figure 1. (A) Cast from an LSZ−SWNT supernatant added to PVA with a final film concentration of 34−4.5−61 wt % (27−4.2−69 vol %). (B) Cast from an aqueous LSZ−SWNT mixture added to PVA with a final film concentration of 4.5−9.0−45 wt % (38−8.8−53 vol %). Scalebars are 3 cm. Auburn University logo used with permission from Auburn University.

Figure 2 shows the ATR-FTIR spectra of the mixture and supernatant LSZ−SWNT−PVA films. The film spectra were compared to individual ATR-FTIR spectra of dried SWNT, LSZ, and PVA. The film spectra contained LSZ's characteristic amide I (~1650 cm^{-1}) and amide II (~1535 cm^{-1}) peaks. The film spectra also contained several peaks due to the presence of PVA which exhibits strong peaks at the following absorbances: ~3300 cm^{-1} due to hydroxyl groups, −OH; ~2950 cm^{-1} due to C−H stretch in alkyl chains; C−H in-plane bending at ~1430 cm^{-1}; and ~1050 cm^{-1} due to C−O−H stretch.[15] The films showed increasing absorbance from ~1500 to ~700 cm^{-1} which was also seen for pristine SWNTs. A primary indication

Received: July 30, 2013
Accepted: December 16, 2013
Published: December 30, 2013

   dx.doi.org/10.1021/mz400395j | *ACS Macro Lett.* 2014, 3, 77−79

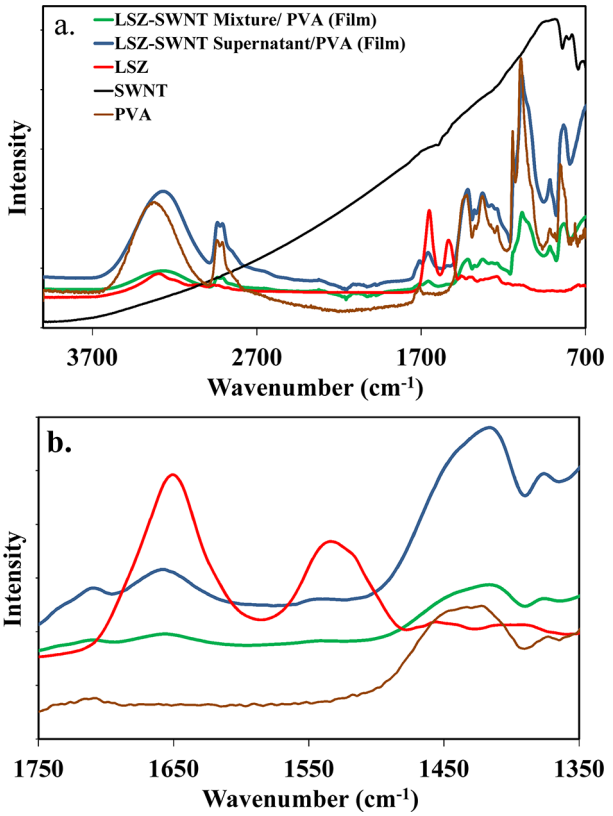

Figure 2. ATR-FTIR spectra (a) covering the entire frequency range scanned and (b) of an enlarged section showing the amide I (1650 cm^{-1}) and II (1535 cm^{-1}) peaks of all LSZ-containing samples.

of the presence of interactions rather than separate individual components was the red or blue shifting of peaks relative to their pure components; the shifts were slightly more pronounced in the supernatant films than in the mixture films. For example, Figure 2a shows the PVA peak centered at 3333 cm^{-1}, and the LSZ peak at 3307 cm^{-1} resulted in a broad peak centered at 3273 cm^{-1} in the mixture film and a more intense, slightly more shifted, peak in the supernatant films. Similarly, Figure 2b highlights differences in the amide peaks. These shifts are attributed to changes in molecular orientation resulting from changes in the polarity of the environment associated with dispersion in a multicomponent aqueous system.[5,6,15,16]

The retention of LSZ antibacterial activity in the composite films was characterized using a standard turbidimetric analysis based on the lysis of *Micrococcus lysodeikticus* which follows Michaelis–Menten kinetics.[17] The activity was calculated according to the equation

$$\text{Activity} = \frac{(\Delta \text{Abs}_{450}/t)_{\text{test}} - (\Delta \text{Abs}_{450}/t)_{\text{blank}}}{(0.001)(m_{\text{LSZ}})}$$

where ΔAbs_{450} is the change in absorbance intensity, t the kinetic test duration, and m_{LSZ} the mass of LSZ, and test or blank indicates the presence of the active film or the blank buffer solution, respectively. Figure 3 shows the change in absorbance with time for the mixture and supernatant films. As shown in Table 1, the supernatant maintained 84% of LSZ's native LSZ activity, whereas the mixture maintained 53%. This difference in activity was likely due to the differences in the surface to volume ratio for the bundled SWNTs in the mixture

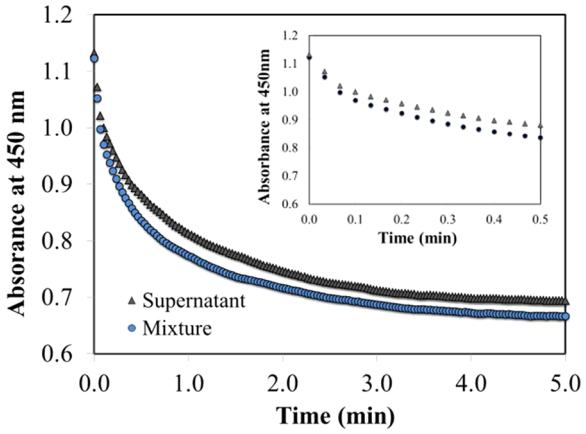

Figure 3. Turbidimetric analysis of mixture and supernatant films. The linear cell death region was based on the first 0.5 min of data shown in the inset.

Table 1. Specific Activity of the Films[a]

	mixture film	supernatant film
linear cell death slope	0.47	0.42
specific activity (active units/mg LSZ)	2950	4620
native LSZ activity maintained (%)	53	84

[a]The native activity of LSZ was 5525 units/mg LSZ, and the LSZ lytic rate was 0.001 abs/min/active unit.

and the individuals in the supernatant as well as differences in the amount of bound and unbound LSZ.

Film tensile testing showed that the presence of SWNTs enhanced film mechanical strength by up to eight times. As shown in Table 2, in spite of the presence of visible aggregates, the mixture films had a six times greater Young's modulus and a 20% increase in tensile strength than the control films prepared in the absence of SWNTs. For the supernatant films, the Young's modulus was over eight times greater than the control and over 30% higher than the mixture film. This was in spite of the SWNT concentration in the supernatant films being half that of the mixture films. Similarly, the tensile strength of the supernatant films was 73% higher than the control and 39% higher than the mixture films. These results highlight that dispersion state can be a more important determinant of mechanical properties than composition. In addition to the visible aggregates creating obvious defects, which limit tensile strength, individuals have greater specific surface area and therefore more interfacial interactions with the matrix and greater reinforcement potential.[18]

The methods used in this research provide a foundation for the production of other bulk composites from enzymes and nanomaterials. The addition of PVA to LSZ–SWNT dispersions enabled higher concentrations and the production of cast films. The films combined LSZ's antibacterial properties with the mechanical properties of SWNT and PVA. The best mechanical properties were achieved for films produced from concentrated supernatants; this highlights the important effect dispersion state has on mechanical properties.

EXPERIMENTAL SECTION

Materials. SWNT batch CG200-L014 produced by Southwest Nano Technologies (Norman, OK) was used in this research. These SWNTs were made by a catalytic method using cobalt and molybdenum and were 93.4% carbon based on TGA. This process

dx.doi.org/10.1021/mz400395j | ACS Macro Lett. 2014, 3, 77–79

Table 2. Mechanical Properties of Control LSZ−PVA Films and Both Mixture and Supernatant LSZ−SWNT−PVA Films

sample	Young's modulus (MPa)	tensile strength (MPa)	tensile strain (%)
Control Film: 47−53 wt % LSZ−PVA	490 ± 51	69 ± 4.8	27 ± 0.28
Mixture Film: 45−9.0−45 wt % LSZ−SWNT−PVA	3100 ± 34	86 ± 1.9	6.7 ± 0.77
Supernatant Film: 34−4.5−61 wt % LSZ−SWNT−PVA	4100 ± 270	120 ± 4.3	12 ± 0.90

results in a narrow diameter distribution of SWNTs with an average diameter of 1.36 nm. Dialyzed, lyophilized LSZ from hen-egg white was purchased from Sigma Aldrich (St. Louis, MO) and used as delivered. Hydrolyzed PVA with an average molecular weight of 195 000 g/mol and 99.3% purity was also purchased from Sigma Aldrich and used as received. All solutions and dispersions were made using deionized water. The following densities were used for converting between wt % and vol %: 1.45 g/cm^3 SWNT, 1.68 g/cm^3 LSZ, and 1.00 g/cm^3 H_2O.

Sample Preparation. For the mixture films, a dispersion consisting of 200.5 mg of LSZ and 100 mL of deionized water was allowed to mix for 5 min before adding 40.02 mg of SWNT. To disperse the SWNT, the solution was tip sonicated in an ice bath set to an amplitude of 60% for 30 min with pulses of 5 s on and 2 s off. The dispersion was mixed with 5 wt % PVA in water to result in a dispersion of 0.13/0.03/1.60 wt % LSZ−SWNT−PVA (0.08/0.02/1.30 vol %). These dispersions were magnetically stirred for 20 min. The dispersions were then placed on an orbital mixer and allowed to slowly evaporate under ambient conditions to one-fourth of their initial volumes. For the supernatant films, a similar procedure was followed. However, 501.6 mg of LSZ was added to 100 mL of deionized water and mixed for 5 min prior to adding 100.63 mg of SWNT. After sonication, the dispersion was first centrifuged for 3 h at 17 000*g*, and only the supernatant was retained. The removal of the bundles and aggregates by centrifugation resulted in 0.61/0.04 wt % LSZ−SWNT (0.36/0.03 vol %); this was added to PVA solution using magnetic stirring resulting in a 0.47/0.03/1.10 wt % LSZ/SWNT/PVA (0.28/0.02/0.91 vol %) dispersion. Dispersion concentrations were determined using UV−vis calibration curves.[3] As for the mixtures, the dispersions produced from the supernatants were concentrated 4-fold by slow evaporation on an orbital mixer. Films were then cast onto a 6 in. diameter flat-bottom glass dish. The dispersions were evenly spread over the entire bottom of the dish and allowed to dry on an orbital mixer in a fume hood. A TA Instruments (New Castle, DE) Q50 TGA coupled to a Nicolet (Waltham, MA) FTIR was used to determine the amounts of each component. FTIR spectra for examining interactions were obtained using an attenuated total reflectance (ATR) method with a germanium crystal. Each sample run consisted of 64 scans from 500 to 3700 cm^{-1}.

Turbidimetric Analysis. A Cary (United States) 3E UV−vis spectrophotometer was used to determine antibacterial activity based on lysis of *Micrococcus lysodeikticus* according to the procedure from Sigma Aldrich. A 66 mM solution of potassium phosphate buffer was adjusted to a pH of 6.24 with potassium hydroxide at room temperature. A bacterial cell suspension in the potassium phosphate buffer containing 0.015 wt % *Micrococcus lysodeikticus* was then prepared. Quartz cuvettes with a 1 cm path length were filled with 2.5 mL of the bacterial suspension, and 0.1 mL of buffer solution or liquid dispersions was added. UV−vis was then performed on the buffer solution and the bacterial suspension containing the films. Kinetic scans were run at 450 nm for 5 min.

Mechanical Testing. An Instron 5565 Calibration Lab (Norwood, MA) was used to determine film mechanical properties. Films were cut and then glued into a paper testing frame with a gauge length of 26 mm. The load cell used for this testing was 100 cN with a cross-head speed of 1.0 mm/min. The load and gauge length were balanced and zeroed before each run.

AUTHOR INFORMATION

Corresponding Author

*E-mail: davisva@auburn.edu. Tel.: (334) 844-2060.

Notes

The authors declare no competing financial interest.

ACKNOWLEDGMENTS

Funding was provided by the National Science Foundation CAREER/PECASE Award − CMMI 0846629 and an associated Research Experience for Undergraduates supplement.

REFERENCES

(1) Badaire, S.; Zakri, C.; Maugey, M.; Derre, A.; Barisci, J. N.; Wallace, G.; Poulin, P. *Adv. Mater.* **2005**, *17*, 1673.
(2) Ao, G.; Nepal, D.; Aono, M.; Davis, V. A. *ACS Nano* **2011**, *5*, 1450.
(3) Nepal, D.; Balasubramanian, S.; Simonian, A. L.; Davis, V. A. *Nano Lett.* **2008**, *8*, 1896.
(4) Nepal, D.; Minus, M. L.; Kumar, S. *Macromol. Biosci.* **2011**, *11*, 875.
(5) Xie, L. M.; Chou, S. G.; Pande, A.; Pande, J.; Zhang, J.; Dresselhaus, M. S.; Kong, J.; Liu, Z. F. *J. Phys. Chem. C* **2010**, *114*, 7717.
(6) Horn, D. W.; Tracy, K.; Easley, C. J.; Davis, V. A. *J. Phys. Chem. C* **2012**, *116*, 10341.
(7) Matsuura, K.; Saito, T.; Okazaki, T.; Ohshima, S.; Yumura, M.; Iijima, S. *Chem. Phys. Lett.* **2006**, *429*, 497.
(8) Mantha, S.; Pedrosa, V. A.; Olsen, E. V.; Davis, V. A.; Simonian, A. L. *Langmuir* **2010**, *26*, 19114.
(9) Tenovuo, J. *Oral Dis.* **2002**, *8*, 23.
(10) Hannig, C.; Hoch, J.; Becker, K.; Hannig, M.; Attin, T. *Arch. Oral Biol.* **2005**, *50*, 821.
(11) Hannig, C.; Spitzmüller, B.; Lux, H. C.; Altenburger, M.; Al-Ahmad, A.; Hannig, M. *Arch. Oral Biol.* **2010**, *55*, 463.
(12) Duan, J.; Park, S. L.; Daeschel, M. A.; Zhao, Y. J. *Food Sci* **2007**, *72*, M355.
(13) Poulin, P.; Vigolo, B.; Launois, P. *Carbon* **2002**, *40*, 1741.
(14) Bomboi, F.; Bonincontro, A.; La Mesa, C.; Tardani, F. J. *Colloid Interface Sci.* **2011**, *355*, 342.
(15) Mansur, H. S.; Oréfice, R. L.; Mansur, A. A. P. *Polymer* **2004**, *45*, 7193.
(16) Nepal, D.; Geckeler, K. E. *Small* **2006**, *2*, 406.
(17) Sigma-Aldrich, Enzymatic Activity of Lysozyme (Ec 3.2.1.17); Vol. 2012.
(18) Zhang, X.; Liu, T.; Sreekumar, T. V.; Kumar, S.; Moore, V. C.; Hauge, R. H.; Smalley, R. E. *Nano Lett.* **2003**, *3*, 1285.